JOURNAL OF GUIDANCE, CONTROL, AND DYNAMICS
Vol. 28, No. 3, May–June 2005

Engineering Notes

ENGINEERING NOTES are short manuscripts describing new developments or important results of a preliminary nature. These Notes should not exceed 2500 words (where a figure or table counts as 200 words). Following informal review by the Editors, they may be published within a few months of the date of receipt. Style requirements are the same as for regular contributions (see inside back cover).

Control Law for Active Structural Damping Using a Control Moment Gyro

Jian-Feng Shi* and Christopher J. Damaren†
University of Toronto, Toronto, Ontario M3H 5T6, Canada

I. Introduction

SPINNING wheels have long been used as torque actuators in spacecraft applications. A constant speed wheel with variable spin axis is usually termed a control moment gyro (CMG).[1] A single-gimbaled CMG (SGCMG) is created when the CMG is mounted in a gimbal and motors are used to spin the wheel about the spin axis and produce gimbal motion about the gimbal axis. The output torque is about an axis perpendicular to the spin and gimbal axes.

Most of the research on CMGs has concentrated on their use for attitude control[2] and methods for generating the gimbal rates given the desired output torques. There have been few studies employing the CMG for active damping. This is somewhat surprising because the CMG is a clean actuator (i.e., no plume impingements) exhibiting a control torque that varies linearly with gimbal rate. Active damping is a requirement on flexible spacecraft where oscillations can develop from, for example, slewing maneuvers or solar-array thermal snap. A device termed the gyrodamper was introduced by Aubrun and Margulies.[3] It consisted of a SGCMG with an angular rate sensor that measured the inertial angular rate about the output torque axis. They noted that the use of a constant proportional gain between the angular rate and the gimbal rate (hence output torque) would mimic a purely passive rotational dashpot.

Since the appearance of Ref. 3, there have been a few studies using the CMG for active damping. These include Ref. 4, where a SGCMG was placed at the tip of a pendulum to dampen its motion, and Ref. 5, where a very large SGCMG was used to dampen the oscillatory motions of a gondola. Bauer[6] and Muise and Bauer[7] have examined the design and control of a double-gimbaled CMG for active damping. In their work, the performance of the double-gimbaled CMG is compared with that of the SGCMG for damping out the vibration of a beam.

This Note investigates the use of a SGCMG whose output torque axis is nominally collocated with an angular velocity sensor and is located at the end of a cantilevered beam. Furthermore, it has been constructed so that the gimbal travel is restricted to ±20 deg. This leads to an easier mechanical design and also ensures that the output torque axis is roughly constant and remains aligned with the rate sensor axis. It is demonstrated that direct angular velocity feedback with a proportional gain is not consistent with zeroing the gimbal angle. A modification to the feedback law, which incorporates an additional gimbal angle feedback term, is shown to make the gimbal angle go to the zero reference asymptotically. This is important when using a device that has been constructed with limited gimbal travel leading to an approximately constant output torque axis. Experimental results illustrate this property and demonstrate the active damping that can be achieved.

Received 2 June 2004; revision received 23 September 2004; accepted for publication 13 October 2004.

*M.S. Candidate, Institute for Aerospace Studies, 4925 Dufferin Street.
†Associate Professor, Institute for Aerospace Studies, 4925 Dufferin Street. Senior Member AIAA.

II. Control Law Development

A. Dynamics of a Flexible Structure Containing a CMG

In this section, we consider a flexible structure that is constrained to prevent rigid-body motion and whose configuration is described by a column of generalized coordinates $\boldsymbol{q}(t)$. It is assumed that the kinetic energy can be written as

$$T_1 = \tfrac{1}{2}\dot{\boldsymbol{q}}^T \boldsymbol{M}\dot{\boldsymbol{q}} \tag{1}$$

where $\boldsymbol{M} = \boldsymbol{M}^T > \boldsymbol{O}$ is the mass matrix. The strain energy is assumed to be of the form

$$U = \tfrac{1}{2}\boldsymbol{q}^T \boldsymbol{K}\boldsymbol{q} \tag{2}$$

where $\boldsymbol{K} = \boldsymbol{K}^T > \boldsymbol{O}$ is the stiffness matrix.

We now embed a SGCMG into the flexible structure (Fig. 1). A reference frame $\mathcal{F}_t$ is also embedded at this location whose 1 axis is aligned with the spin axis for zero gimbal motion $\beta_g(t)$, the 2 axis is aligned with the gimbal axis, and the 3 axis completes the right-handed system. It is assumed that the angular momentum stored in the wheel is $h_s = I_s\omega_s \geq 0$, where ω_s is the constant wheel speed and I_s is the spin moment of inertia. It is assumed that the mass properties associated with the nonspinning CMG are already included in the mass matrix $\boldsymbol{M}$. The additional kinetic energy imparted by the spinning wheel with moving gimbal is

$$T_2 = \boldsymbol{h}_s^T\boldsymbol{\omega} + \tfrac{1}{2}I_s\omega_s^2$$

Here, $\boldsymbol{h}_s$ is the stored angular momentum vector expressed in $\mathcal{F}_t$, which for small gimbal motions can be written as

$$\boldsymbol{h}_s = [h_s \quad -h_s\beta_g(t) \quad 0]^T$$

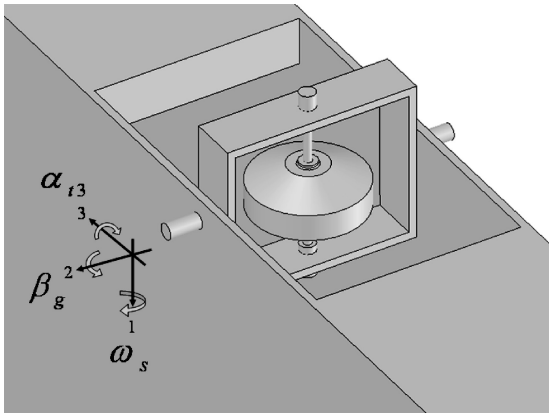

Fig. 1 SGCMG embedded in a flexible structure.

The column $\boldsymbol{\omega}$ denotes the angular velocity of $\mathcal{F}_t$ expressed in $\mathcal{F}_t$. If $\mathcal{F}_t$ is rotated from its undeformed position by three small rotations $\boldsymbol{\alpha}_t = [\alpha_{t1} \;\; \alpha_{t2} \;\; \alpha_{t3}]^T$ as a result of elastic deformation, then the angular velocity, to second order, can be expressed as

$$\boldsymbol{\omega} = \left(1 - \tfrac{1}{2}\boldsymbol{\alpha}_t^{\times}\right)\dot{\boldsymbol{\alpha}}_t$$

Therefore, to second order, the spin kinetic energy can be written as

$$T_2 = h_s\dot{\alpha}_{t1} - h_s\beta_g(t)\dot{\alpha}_{t3} + \tfrac{1}{2}h_s(\alpha_{t3}\dot{\alpha}_{t2} - \alpha_{t2}\dot{\alpha}_{t3}) + \tfrac{1}{2}I_s\omega_s^2 \quad (3)$$

If it is assumed that the elastic rotations can be written as $\alpha_{ti} = \boldsymbol{\psi}_i^T\boldsymbol{q}$, $i = 1, 2, 3$, for constant columns $\boldsymbol{\psi}_i$, then

$$T_2 = h_s\boldsymbol{\psi}_1^T\dot{\boldsymbol{q}} - \beta_g(t)h_s\boldsymbol{B}^T\dot{\boldsymbol{q}} + \tfrac{1}{2}\dot{\boldsymbol{q}}^T\boldsymbol{G}\boldsymbol{q} + \tfrac{1}{2}I_s\omega_s^2$$

where $\boldsymbol{B} = \boldsymbol{\psi}_3$ and $\boldsymbol{G} = h_s[\boldsymbol{\psi}_2\boldsymbol{\psi}_3^T - \boldsymbol{\psi}_3\boldsymbol{\psi}_2^T] = -\boldsymbol{G}^T$. In addition to the preceding energy expressions, we assume that the presence of structural damping leads to a nonconservative virtual work given by $\delta W_e = -\delta\boldsymbol{q}^T\boldsymbol{D}\dot{\boldsymbol{q}}$, where $\boldsymbol{D} = \boldsymbol{D}^T > \boldsymbol{O}$. Applying Hamilton's (extended) principle to the kinetic energy $T = T_1 + T_2$, the strain energy U, and δW_e leads to the motion equation

$$\boldsymbol{M}\ddot{\boldsymbol{q}} + (\boldsymbol{D} + \boldsymbol{G})\dot{\boldsymbol{q}} + \boldsymbol{K}\boldsymbol{q} = \boldsymbol{B}h_s\dot{\beta}_g(t) \quad (4)$$

Now, consider the Lyapunov function

$$H(t) = \tfrac{1}{2}\dot{\boldsymbol{q}}^T\boldsymbol{M}\dot{\boldsymbol{q}} + \tfrac{1}{2}\boldsymbol{q}^T\boldsymbol{K}\boldsymbol{q} \geq 0 \quad (5)$$

We have

$$\dot{H} = -\dot{\boldsymbol{q}}^T\boldsymbol{D}\dot{\boldsymbol{q}} + h_s\dot{\beta}_g\boldsymbol{B}^T\dot{\boldsymbol{q}} \quad (6)$$

where it is noted that $\dot{\alpha}_{t3} = \boldsymbol{B}^T\dot{\boldsymbol{q}}$ is the angular velocity collocated with the CMG output torque axis. Equations (5) and (6) can be used to demonstrate the passivity property[8] that exists between the input $\dot{\beta}_g$ and the output $\dot{\alpha}_{t3}$. It is well known that such a system can be stabilized using a strictly positive real control system connected in negative feedback.[9] In the present case, the simplest implementation is a straight feedback gain

$$\dot{\beta}_g = -k_d\dot{\alpha}_{t3}, \qquad k_d > 0$$

which leads to

$$\dot{H} = -\dot{\boldsymbol{q}}^T\boldsymbol{D}\dot{\boldsymbol{q}} - h_sk_d\dot{\boldsymbol{q}}^T\boldsymbol{B}\boldsymbol{B}^T\dot{\boldsymbol{q}} \leq 0$$

Using LaSalle's theorem, the system in Eq. (4) coupled with the feedback law is asymptotically stable. This also follows when $\boldsymbol{D} = \boldsymbol{O}$ if the system is observable using the output $\dot{\alpha}_{t3} = \boldsymbol{B}^T\dot{\boldsymbol{q}}$.

Integrating the feedback law leads to $\beta_g(t) = \beta_g(0) - k_d[\alpha_{t3}(t) - \alpha_{t3}(0)]$. If $\beta_g(0) = 0$, then the asymptotic stability implies that

$$\lim_{t\to\infty}\beta_g(t) = k_d\alpha_{t3}(0)$$

so that, in general, the gimbal angle does not tend to zero. In the interest of keeping the gimbal angle small, it would be desirable if $\beta_g(t)$ could be made to asymptotically tend to the zero reference. To this end, we introduce the modified feedback law

$$\dot{\beta}_g(t) = -k_d\dot{\alpha}_{t3} - k_b\beta_g(t) \quad (7)$$

with $k_b > 0$. Taking Lapace transforms, we have

$$\dot{\beta}_g(s)/\dot{\alpha}_{t3}(s) = -k_ds/(s + k_b) = -G_c(s) \quad (8)$$

Hence, the control law is equivalent to replacing the direct angular velocity feedback with a high-pass filter $G_c(s) = k_ds/(s + k_b)$. In the actual controller implementation, Eq. (7) is used to determine the desired gimbal rate using actual gimbal angle feedback; high-pass filtering of the angular rate measurement is not used although it is mathematically equivalent. We note that $G_c(s)$ is analytic in the closed right-half plane and $Re\{G_c(j\omega)\} = k_d\omega^2/(\omega^2 + k_b^2) \geq 0$. Hence, $G_c(s)$ is positive real but not strictly positive real.[10] However, we can still demonstrate asymptotic stability with respect to the structural motion and gimbal motion.

Let us define $u(t) = \dot{\beta}_g$, $y(t) = \dot{\alpha}_{t3}$, $Q = k_b/k_d$, $M = k_b/\sqrt{k_d}$, and $N = \sqrt{k_d}$. Adopting the Lyapunov function

$$V(t) = H(t) + \tfrac{1}{2}h_sQ\beta_g^2(t) \geq 0$$

we have, using Eqs. (6) and (7),

$$\begin{aligned}
\dot{V} &= \dot{H} + h_sQ\beta_g\dot{\beta}_g \\
&= -\dot{\boldsymbol{q}}^T\boldsymbol{D}\dot{\boldsymbol{q}} + h_s\dot{\boldsymbol{q}}^T\boldsymbol{B}u - h_sQ\beta_g(k_b\beta_g + k_dy) \\
&= -\dot{\boldsymbol{q}}^T\boldsymbol{D}\dot{\boldsymbol{q}} + h_syu - h_s(M\beta_g)^2 - h_sk_b\beta_gy \\
&= -\dot{\boldsymbol{q}}^T\boldsymbol{D}\dot{\boldsymbol{q}} - h_sy(k_b\beta_g + k_dy) - h_s(M\beta_g)^2 - h_sk_b\beta_gy \\
&= -\dot{\boldsymbol{q}}^T\boldsymbol{D}\dot{\boldsymbol{q}} - h_s(M\beta_g)^2 - 2h_sMN\beta_gy - h_sN^2y^2 \\
&= -\dot{\boldsymbol{q}}^T\boldsymbol{D}\dot{\boldsymbol{q}} - h_s(M\beta_g + Ny)^2 \leq 0
\end{aligned}$$

Clearly, we have Lyapunov stability and applying LaSalle's theorem, the invariant set contains $\dot{\boldsymbol{q}} = 0$ and $M\beta_g(t) + Ny(t) = 0$. Because, $\dot{\boldsymbol{q}} = 0$, it follows that $y = \boldsymbol{B}^T\dot{\boldsymbol{q}} = 0$; hence, $\beta_g = 0$. Therefore, $u = 0$; hence, $\boldsymbol{K}\boldsymbol{q} = 0$ implying $\boldsymbol{q} = 0$. Thus, the system is globally asymptotically stable. This result is indicative of robust stability because it does not rely on the specific values of $\boldsymbol{M}$, $\boldsymbol{D}$, $\boldsymbol{G}$, or $\boldsymbol{K}$ but only on their definiteness and symmetry properties, which depend only on the dynamical principles.

B. CMG Gimbal Motor Control Law

Denote the desired gimbal rate produced by the feedback law in Eq. (7) by $\dot{\beta}_d$, and let $\dot{\beta}_g$ continue to denote the actual gimbal rate. In our experimental setup, the gimbal axis is driven by a brushed dc motor driving through a gearbox. The motor is controlled by varying the armature voltage denoted by $V_g(t)$. The dc motor is described by the equation $V_g = R_ai_a + K_e\dot{\beta}_g$, where R_a is the armature resistance, i_a is the armature current, K_e is the back electromotive force (EMF) constant, and we have neglected the armature inductance. The motor output torque is given by $\tau = K_ti_a$, where K_t is the motor torque constant. One possibility for making the gimbal rate track its desired value is the use of a closed-loop feedback law where the armature voltage is, for example, a proportional–integral (PI) function of the tracking error. This requires the use of potentially noisy gimbal rate measurements. We have adopted an open-loop sensorless approach where the armature voltage is given by $V_g(t) = K_e\dot{\beta}_d(t)$. Combining this with the preceding two relationships for the motor dynamics, we arrive at the following expression for the motor torque:

$$\tau = K_ti_a = -(K_tK_e/R_a)(\dot{\beta}_g - \dot{\beta}_d)$$

Hence, this approach is equivalent to using an error-driven proportional feedback law for the motor torque where the back EMF has furnished the (noiseless) gimbal rate measurement. If we neglect friction, then the gimbal torque can be approximately related to the gimbal motion by $I_g\ddot{\beta}_g = \tau$, where I_g is the moment of inertia of the gimbal axis assembly about the gimbal axis. When this is combined with the preceding torque expression, the closed-loop transfer function relating the desired gimbal rate to the true gimbal rate can be written as $\dot{\beta}_g(s)/\dot{\beta}_d(s) = a/(s + a)$, where $a = K_eK_t/(I_aR_a)$. In our application, the cutoff frequency a is much larger than the frequencies of the vibration modes that we seek to dampen.

III. Experimental Results

A SGCMG with collocated angular rate sensor was designed and built at the University of Toronto Institute for Aerospace Studies. A schematic representation of the SGCMG is shown in Fig. 2. The spin axis is controlled using a brushless dc motor, and the gimbal axis is driven with a brushed dc motor. The rate sensor is a Systron-Donner QRS-11 inertial rate sensor. The spin motor speed is measured by counting pulses generated by a Hall effect sensor on one of the motor phases. There is a quadrature encoder and an analog potentiometer on the gimbal axis. The gimbal motor gearbox ratio is 449.1:1, and the armature voltage is created using a pulse-width-modulation (PWM) signal with a frequency of 187.5 kHz. The spin motor phases were driven with a constant duty cycle PWM voltage signal so that the rotor spin rate was 4000 rpm. Open-loop control of the spin motor has been used. We compared this with closed-loop control (a PI law) of the spin motor, and the regulation was comparable. For one test we performed with a commanded spin rate of 4000 rpm,

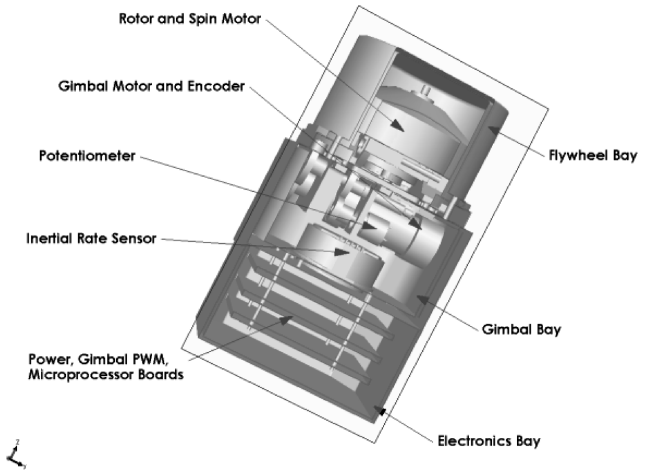

Fig. 2 SGCMG prototype.

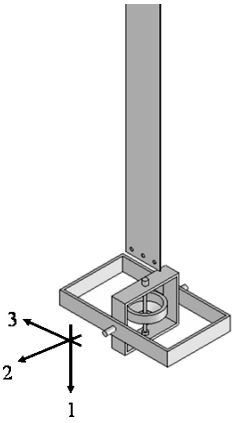

Fig. 3 Gyrodamper and beam system (schematic).

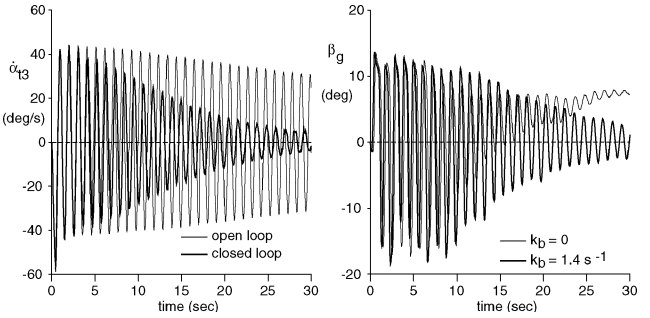

Fig. 4 Rate sensor and gimbal angle response.

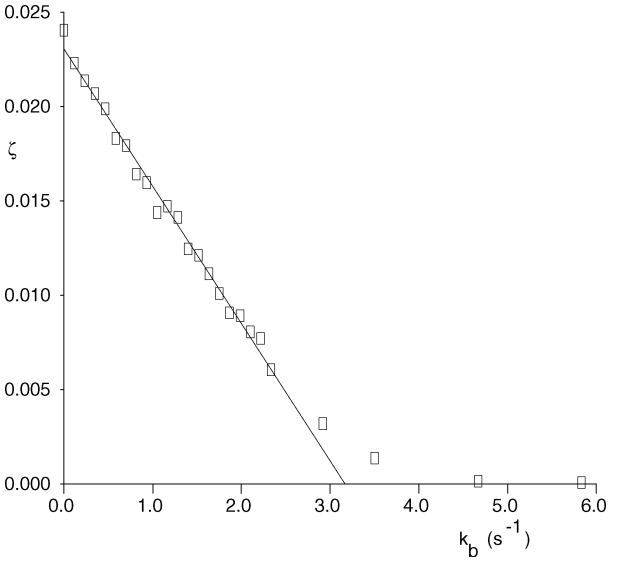

Fig. 5 Damping ratio vs gimbal angle feedback gain ($k_d = 3.05$).

the open-loop mode produced a spin rate of 4011 ± 18 rpm, and the closed-loop mode produced a spin rate of 4000 ± 20 rpm. The data given here are the mean value and 1-σ variation.

The electronics is self-contained within the device and is capable of managing power, gimbal motor PWM, and real-time computations. A 16-MHz microprocessor (the Siemens C164CI) was used. The assembled device is contained within an aluminum enclosure with dimensions $86 \times 86 \times 155$ mm. The mass of the entire device is $m_g = 1.267$ kg. The spin inertia is $I_s = 2.08 \times 10^{-4}$ kg $\cdot$ m^2, which yields a stored angular momentum of 8.71×10^{-2} N $\cdot$ m $\cdot$ s. When multiplied by the maximum gimbal rate that can be sensed (60.4 deg/s), the maximum control torque that can be achieved is 92 mN $\cdot$ m. The properties of the gimbal motor are $K_e = K_t = 4.913$ V $\cdot$ s/rad, $R_a = 14.1\Omega$, and $I_g = 1.5 \times 10^{-4}$ kg $\cdot$ m^2.

The analog potentiometer and the rate sensor are interfaced to 10-bit (with sign) analog-to-digital converters. For the potentiometer, 1 count $= 0.0716$ deg, and the noise was less than ± 1 count. For the rate sensor, 1 count $= 0.118$ deg/s, and the noise was on the order of ± 1 count. The rate sensor exhibited a repeatable dc bias of -9 counts, which was easily removed. Both sensors are sampled by the microprocessor at a rate of 30 Hz and have low-pass analog filtering with a cutoff of 15 Hz.

This device that we have termed the GyroDamper has been attached to the end of a clamped-free cantilevered beam, which is suspended vertically. The beam is 0.5 m long and is made of aluminum with a cross section that is 76.2×1.59 mm. A schematic representation is shown in Fig. 3. The moment of inertia of the GyroDamper about the beam attachment axis is $J_g = 9.15 \times 10^{-3}$ kg $\cdot$ m^2, and its first moment of mass about this axis is $c_g = 0.108$ kg $\cdot$ m.

For the experimental results to be presented, an impressed tip deflection of 0.127 m with zero rate was the initial condition. The rate sensor output is shown in Fig. 4 for the open-loop case corresponding to zero gimbal and spin motion. The response is dominated by the first mode, which exhibits a damped natural frequency of 1.03 Hz and a damping ratio of $\zeta_{1,o} = 0.0023$.

The closed-loop rate sensor response corresponding to $k_d = 3.05$ and $k_b = 0$ increased the damping ratio to $\zeta_{1,c} = 0.025$. The selected value of k_d is the maximum rate gain that could be selected without saturating the gimbal motor voltage. The gimbal angle is also shown in Fig. 4 ($k_b = 0$), and, as expected, the gimbal angle does not tend to zero. Next, the value of k_b was increased to 1.40 s^{-1} with k_d unchanged. The closed-loop response from the rate sensor and the gimbal angle history are given in Fig. 4. The damping ratio has been reduced to $\zeta = 0.012$, but the gimbal angle now clearly decreases toward zero. A graph of the damping ratio realized in the first vibration mode as a function of the value of k_b is given in Fig. 5. All values were determined experimentally with the fixed value of $k_d = 3.05$. Clearly, the damping ratio falls off monotonically with k_b, and this relationship is linear for k_b sufficiently small. It has already been noted that for $k_b > 0$, the gimbal angle tends to the zero reference asymptotically. Because the effective damping is reduced as k_b increases, one might wonder if there are any advantages to increasing k_b. By examining the gimbal angle trajectories for the various values of k_b, it was noted that the time it takes for the gimbal angle to become "centered" about $\beta_g = 0$ decreases as k_b increases. This time is approximately 15 s in Fig. 4.

IV. Conclusions

Active damping of flexible structures has been examined using a collocated SGCMG and angular rate sensor, referred to here as the GyroDamper. It has been demonstrated mathematically and experimentally that direct feedback between the angular rate sensor and the gimbal rate leads to asymptotic stability but, in general, the gimbal angle does not go to the zero reference asymptotically. A simple modification to the feedback law that incorporates an

additional term proportional to the gimbal angle was shown to remedy this drawback and preserve the robust stability of a straight feedback gain. Experimental results using a prototype GyroDamper mounted to the tip of a cantilevered beam illustrated and agreed with the theory.

Acknowledgments

The authors thank the following individuals for their assistance in realizing the gyrodamper prototype: Mayes Mullins for the mechanical design, Chris Sherman for the gimbal board electronics, Doug Sinclair for integration of the electronics, Ron Wessels for assistance with porting the software, and Kieran Carroll, whose vision initiated the project in the first place.

References

[1]O'Connor, B. J., and Morine, L. A., "A Description of the CMG and Its Application to Space Vehicle Control," *Journal of Spacecraft and Rockets*, Vol. 6, No. 3, 1969, pp. 225–231.

[2]Jacot, A. D., and Liska, D. J., "Control Moment Gyros in Attitude Control," *Journal of Spacecraft and Rockets*, Vol. 3, No. 9, 1966, pp. 1313–1320.

[3]Aubrun, J. N., and Margulies, G., "Gyrodampers for Large Space Structures," NASA CR-159171, Feb. 1979.

[4]Nishihara, O., Matsuhisa, H., and Sato, S., "Vibration Damping Mechanisms with Gyroscopic Moment," *JSME International Journal. Series III. Vibration, Control, Engineering, Engineering for Industry*, Vol. 35, No. 1, 1992, pp. 50–55.

[5]Kanki, H., Nekomoto, Y., Monobe, H., Ogura, H., and Kobayashi, K., "Development of CMG Active Vibration Control Device for Gondola," *JSME International Journal. Series C. Dynamics, Control, Robotics, Design, and Manufacturing*, Vol. 37, No. 3, 1994, pp. 468–470.

[6]Bauer, R. J., "Kinematics and Dynamics of a Double-Gimbaled Control Moment Gyroscope," *Mechanism and Machine Theory*, Vol. 37, No. 12, 2002, pp. 1513–1529.

[7]Muise, A., and Bauer, R. J., "A Comparison of the Effectiveness of Double- and Single-Gimbaled Control Moment Gyroscopes for Vibration Suppression," *Mechanism and Machine Theory* (submitted for publication).

[8]Desoer, C. A., and Vidyasagar, M., *Feedback Systems: Input-Output Properties*, Academic Press, New York, 1975, Chap. 6.

[9]Benhabib, R. J., Iwens, R. P., and Jackson, R. L., "Stability of Large Space Structure Control Systems Using Positivity Concepts," *Journal of Guidance and Control*, Vol. 4, No. 5, 1981, pp. 487–494.

[10]Ioannou, P., and Tao, G., "Frequency Domain Conditions for Strictly Positive Real Functions," *IEEE Transactions Automatic Control*, Vol. 32, No. 1, 1987, pp. 53, 54.